Egyptian Journal of Pure and Applied Science

Plus-Shaped Dielectric Resonator Antenna with Parasitic Rectangular Elements for Multiband Applications

Alaa Yossry[1, 2], Mostafa El-Aasser[2], Ashraf Yahia[2], and Nasr Gad[2, 3]

[1]*Department of Physics, School of Sciences and Engineering, the American University in Cairo, New Cairo, 11835, Egypt.*

[2]*Electronics Group, Physics Department, Faculty of Science, Ain Shams University, 11566, Cairo, Egypt*

[3]*Department of Physics, Faculty of Science, Galala University, New Galala City, 43511, Egypt.*

ARTICLE INFO

Received 1 February 2023
Accepted 12 March 2023

Keywords

Dielectric Resonator Antenna (DRA),
Defected Ground Structure (DGS),
Parasitic Elements,
Wide-bands,
Multi-bands Antenna.

Correspondence

Alaa Yossry

E-mail

alaa_yossry@aucegypt.edu

ABSTRACT

A new Plus-shaped Dielectric Resonator Antenna (DRA) with parasitic rectangular elements (P-DRA) is proposed for multi-band applications. The antenna is made up of a plus-shaped dielectric resonator and four parasitic rectangular elements that create a rectangular antenna with four L-slots. The P-DRA has a relative permittivity of 15 and is mounted on a 50-ohm microstrip feeding line with a partial and defective ground structure. The proposed R-DRA is designed with the dimensions (15 x 12 x 6.4) mm^3. The impedance bandwidth, radiation pattern, return loss, and antenna gain are obtained using an electromagnetic simulator that employs the finite element method. Furthermore, the obtained results are validated by another 3D simulator using the finite integration technique solver. The P-DRA is designed for multiband applications such as sub-7 GHz (4-8 GHz), wireless local area network (WLAN), X-band (9-10) GHz, and (11-12) GHz, and Ku-band (13-16) GHz. The parasitic elements not only contribute to the excitation of additional frequency bands but also enhance the bandwidth of the operating frequencies, providing two broad bands of (4-8) GHz and (13-16) GHz with integrated resonant frequencies.

1. Introduction

In this fast-changing age, dual-band, tri-band, or multiband antennas are necessary to support the growth of various wireless systems. One solution to this trend is the use of multiple antennas, as they improve device functionality and flexibility.

The evolution of microstrip printed patch antennas has led to smaller circuit sizes, and techniques such as the defected structures technique have been used to increase the bandwidth. The two main types of this technique are the defective ground structure (DGS) and the defective microstrip structure (DMS).

The DGS [1] is synthesized using structures like the electromagnetic band gap and is produced by periodic or non-periodic cascading defects in the ground of the substrate plane. The DMS operates similarly but can be inefficient at high frequencies due to increased conductor losses. To solve these losses, dielectric resonator antennas (DRAs) have gained attention in recent years due to their high radiation efficiency, constant gain, ease of excitation, design flexibility, and compact size [2]. Although DRAs come in many shapes, modal analysis is only known for a few basic shapes, such as hemispherical, cylindrical, triangular, and rectangular, with the rectangular shape having one more degree of freedom [3, 4].

Finding a single DRA that covers multiple wireless applications across both low and high-frequency ranges is challenging. Recently, there has been a demand for multiband antennas, and various techniques, such as hybrid antennas that combine DRAs with additional resonating antennas, have been published in the literature [5-8]. To improve DRA performance in multiband applications, either the DMS or DGS can be used at the ground plane, or a combination of both [9], or other techniques such as parasitic elements can be employed to increase the bandwidth of conventional DRAs [10]. With the numerous wireless communication systems available, having a single device that can cover multiple wireless applications is desirable.

The purpose of this article is to introduce a design for a quad-band DRA that uses a parasitic L-shaped element and a microstrip line feed for multiband applications. The designed antenna has dimensions of (30 x 15 x 6.4) mm^3. The hybrid-shape rectangular-DRA (R-DRA) starts with a basic rectangular DRA consisting of a rectangular dielectric resonator material with a relative dielectric constant of ϵ_r = 15, which is fed by a microstrip line of a length calculated based on the substrate dimension [11].

The R-DRA offers more design flexibility than cylindrical DRA because it has three independent geometric dimensions. The design is then improved using the DGS technique to enhance its wideband capability [12]. The final proposed design, a cross-shaped with a middle air gap, is compact and enables four bands to operate simultaneously at four multiband applications such as sub-7 GHz (4-8 GHz), WLAN, X-band (9-10) GHz, (11-12) GHz, and Ku-band (13-16) GHz.

2. ANTENNA DESIGN

Fig. 1 depicts the geometry of the proposed plus-shaped DRA with four parasitic rectangular elements. A single microstrip feed excites the antenna, which has a high permittivity dielectric resonator (DR) and rectangular parasitic elements from the same material with dimension (P1 x P2 = 2.8 x 3.8) mm^2 is located at the top of the substrate at (m, n = 1.2 mm) distance far away from the main plus-shaped DR. Rogers RO3003 substrate with a dimension (L x W = 30 x 15 mm^2) and a thickness (h = 0.76 mm), a dielectric constant (ϵ_r = 3), and a loss tangent (tan δ = 0.0013) support the antenna. A partial ground plane is etched at the bottom metallic surface of the dielectric substrate (Lg x Wg = 12 x 15 mm^2); this partial ground has a slot with dimensions (Ls x Ws = 4 x 1.9 mm^2).

The proposed DRA can be realized using DR with dimensions of length (Ld = 15 mm), width (Wd = 12 mm), thickness (c = 6.4 mm), and middle air gap (a, b, c = 5, 4, 6.4) mm. These dielectric plates are constructed from ECCOSTOCK® HiK material, which has a high dielectric constant (ϵ_r = 15) and a loss tangent (tan δ = 0.002).

A conductive strip (L2 x W1 = 6 x 1.9 mm^2) connected to a microstrip feed line (L1 x W1 = 13 x 1.9 mm^2) excites the DR. With the aid of parametric analyses and an electromagnetic simulator, the suggested low-profile DRA geometry is improved. The proposed antenna's optimized parameters are shown in Table 1.

3. DISCUSSION

Firstly, as reference antenna 1, A basic R-DRA with dimensions of (12 x 15 x 6.4) mm^3 and a relative dielectric constant of ϵ_r = 15 with a loss tangent of tanδ = 0.002 is fed by a 50 Ω rectangular microstrip line with an offset length (L2 = 6 mm) under the dielectric material.

Fig. 2 shows a defected slot on the ground plane with a length (Ls = 4 mm) and a width (Ws = 1.9 mm) to achieve a wideband feature with a small size (a). The R-DRA is analyzed using the dielectric waveguide model [13]. When a block of DR is placed on a dielectric substrate, TE modes are excited, and the fundamental mode's resonant frequency, TE_{111}, is calculated using the following equations [14]

$$f_0 = \frac{c}{2\pi\sqrt{\epsilon_r}}\sqrt{k_x^2 + k_y^2 + k_z^2}, \quad \textbf{(1)}$$

Where

c is the speed of light , ϵ_r is the dielectric constant of DR , a is the length of the DR, $k_x = \frac{\pi}{a}$, $k_Z = \frac{\pi}{2b}$, b is the width of DR

$$c = \frac{2}{k_y} tanh\left(\frac{k_{yo}}{k_y}\right), \quad \textbf{(2)}$$

$$k_{yo} = \sqrt{k_x^2 + k_z^2} \text{ , } c \text{ is the height of } DR$$

Results shown in Fig. 3 indicate that to carry out the plan's ideal scope, antenna1 needs to be modified. Thus, as can be seen in Fig. 2, (b) antenna 2 consequently displays a rectangular air hole that is stacked in the middle of (R-DRA).

The rectangular air gap is optimized using a parametric investigation, and then (a x b) mm^2 air gap (a = 5, b = 3) that was discovered is fixed. After completing the multiband to its full extent, the parasitic elements are provided in two steps to achieve good impedance matching in the upper and lower frequency bands. Fig. 3 depicts the first step, where the vertical element of DSG with optimal dimension (m = 1.2 mm) is introduced to the dielectric resonator, followed by the introduction of a horizontal element with optimal dimension (n =1.2 mm), giving the R-DRA's corners an L-shaped appearance of DGS and creating four parasitic rectangular elements which are non-radiating elements that are placed in front of the radiating plus-DRA to direct the EM wave in its direction. Simulation of the reflection coefficient for the plus-shape DRA case obtained two integrated bandwidths in the range of 4 to 8 GHz, three integrated bandwidths in the range of 13 to 16 GHz, and two frequency bands for $S_{11} \leq$ -10 dB, as shown in Fig. 4.

Every geometrical parameter affects the overall performance of the antenna differently. The effects of parameters on the proposed antenna are investigated in depth in the following section using a 3D electromagnetic simulator based on the finite element method. Fig.4 shows the simulation results of reflection coefficient (S_{11}) verification with another simulator that provides a different solving technique (the finite integration technique). Fig. 5 illustrates the reflection coefficient (S_{11}) of the hybrid-shape R-DRA with various DR heights to investigate the effects of the DR's height.

Fig. 5 illustrates the reflection coefficient (S_{11}) of the hybrid-shape R-DRA with various DR heights to investigate the effects of the DR's height. It is noticed in Fig. 5 that the plus-shaped resonance and impedance bandwidth rise as the height c drops from 9.6 to 3.2 mm. To give a more perfect performance, such as higher gain and efficiency, the proposed plus-shaped DRA is planned at a height of (c = 6.4 mm). By simulating the (S_{11}) of the proposed Plus-shaped DRA with various values of excitation length L2, as shown in Fig. 6, the effects of the feeding mechanism are examined. It is noticed that using the microstrip feed excitation in which a single feed line with its open end is fitted under the DR material, improves the impedance matching of the majority of resounding modes by enabling an effective coupling between the feed mechanism and the DR.

According to Fig. 5, the best impedance matching is achieved when L2 is set to its optimum value of 6 mm. Fig. 6 illustrates the effects of DGS, where the simulation results (S_{11}) of the proposed plus-shaped DRA with the change of the length (Ls) of the DGS slot in the ground show that decreasing (Ls) enhances multiband features and provides better antenna performances when Ls = 4 mm. The proposed plus-shaped DRA offers four bands (4-8 GHz) with two integrated bandwidths (which cover C band and sub 7 GHz applications), (9-10), (11-12) GHz which cover X band applications, and (13-16) GHz which covered Ku band applications for $S_{11} \leq$ -10 dB. Thus, according to the S_{11} simulations, the proposed plus-shaped DRA offers both multiband and wideband features.

4. Conclusion

A multiband plus-shaped dielectric resonator antenna with parasitic rectangular elements (P-DRA) design for various applications is presented in this paper. The proposed P-DRA antenna achieved four frequency bands covering 61.5%, two integrated bandwidths at the range of (4-8) GHz, 10.2%, range (9–10) GHz, 8.5%, range (11–12) GHz, and 20%, three integrated bandwidths with the range (13–16) GHz. The P-DRA assures that the P-DRA is a good option for different applications, including those in the ku band, sub-7 GHz band, satellite communication, and other wireless communication services.

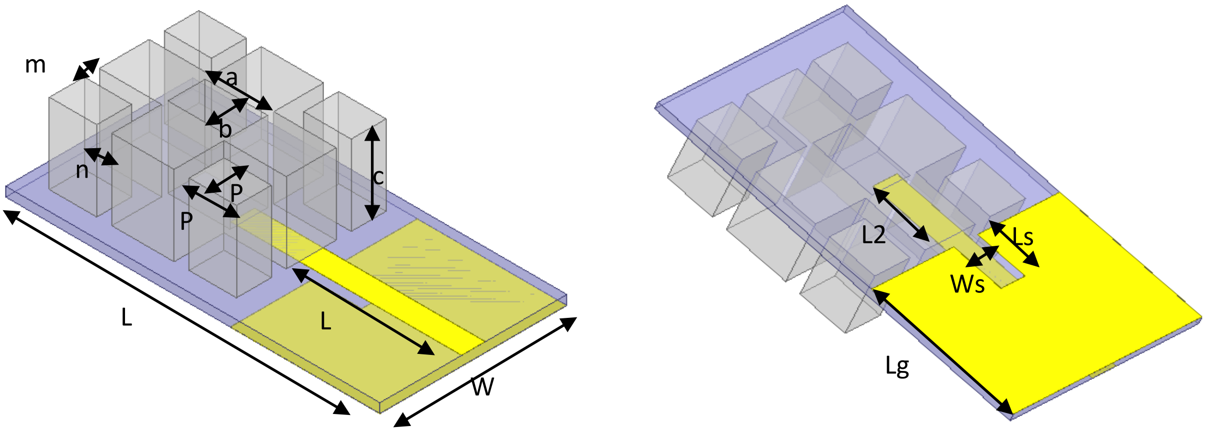

Fig. 1 Geometry of plus-shaped DRA including (top view, bottom view in three-dimensional view)

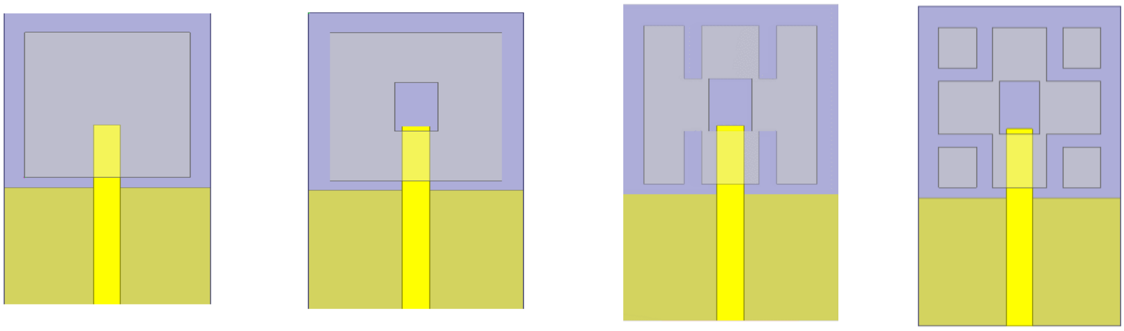

(a) Antenna 1 (b) Antenna 2 (c) Antenna 3 (d) P-DRA with four parasitic elements

Fig. 2 Evaluation of the plus-shaped DRA without (a, b, c) and with four parasitic rectangular elements (d).

Table1. Dimensions of the proposed antenna in mm

Parameters	Dimensions	Parameters	Dimensions
L	30	Lg	12
W = Wg	15	W1=Ws	1.2
L1	13	m = n	1.2
L2	6	a	4
Ws	4	b	5
c	6.4	h	0.76
P1	2.8	P2	3.8

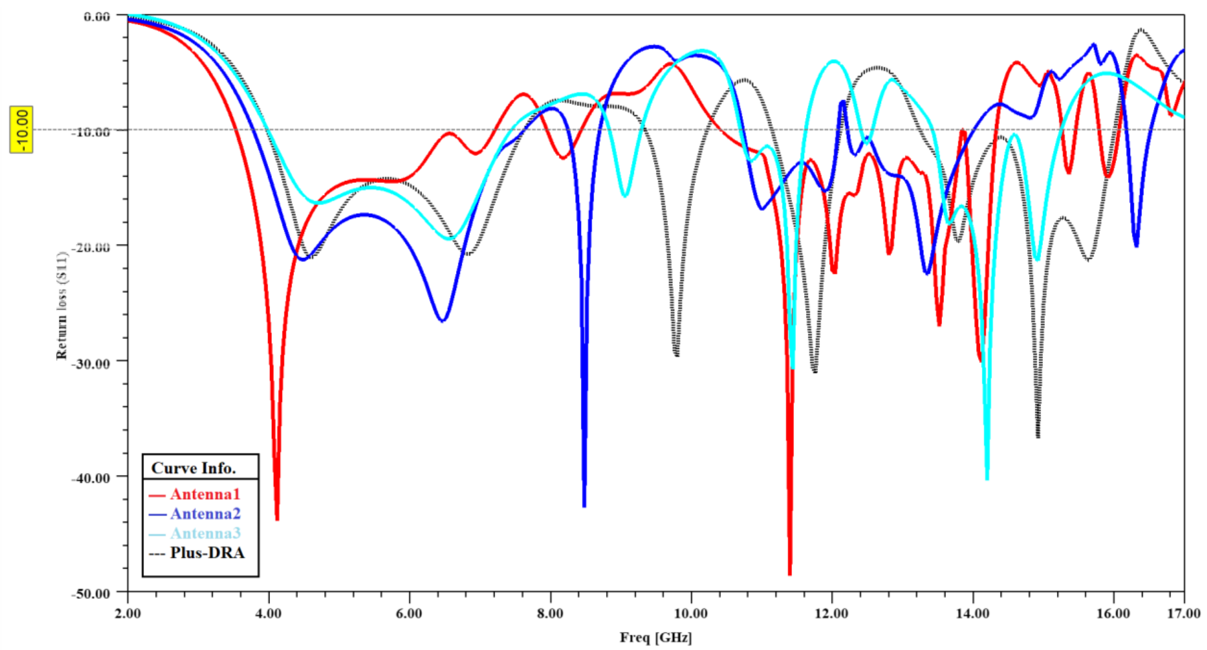

Fig.3 Simulated return loss S_{11} for the case of plus-shaped DRA with four parasitic rectangular elements

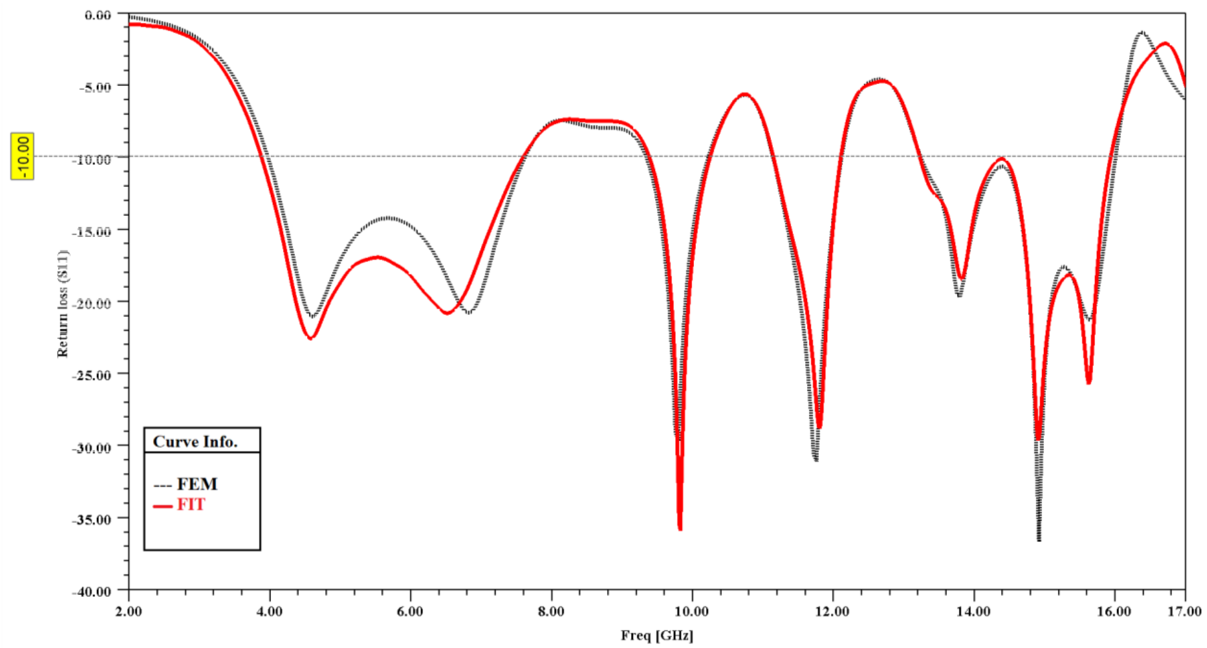

Fig.4 Simulated S_{11} results verification by two simulators using different techniques.

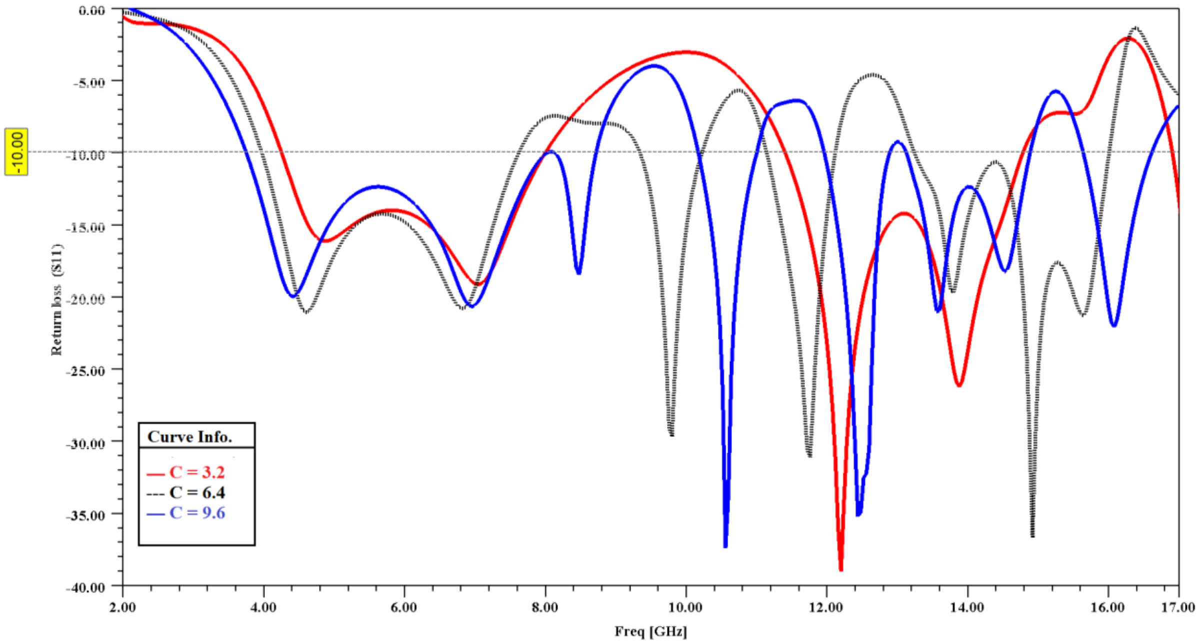

Fig.5 Simulated return loss S_{11} for the P-DRA with various heights of the DR.

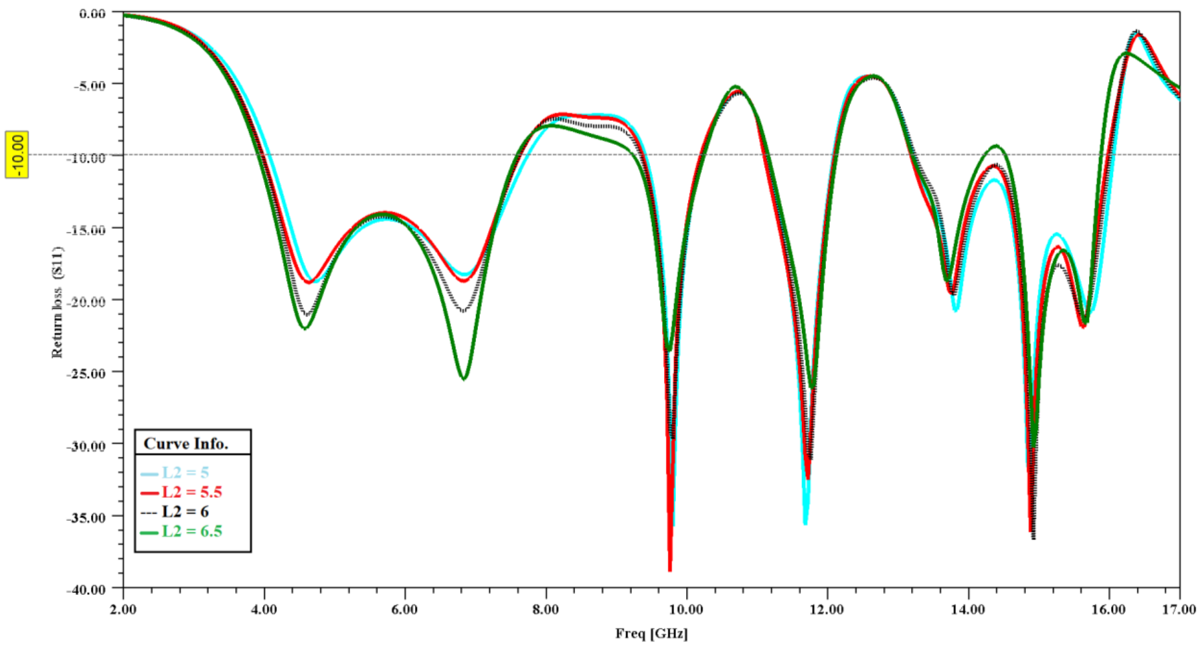

Fig.6 Simulated return loss S_{11} for the P-DRA with different values of the excitation length L2.

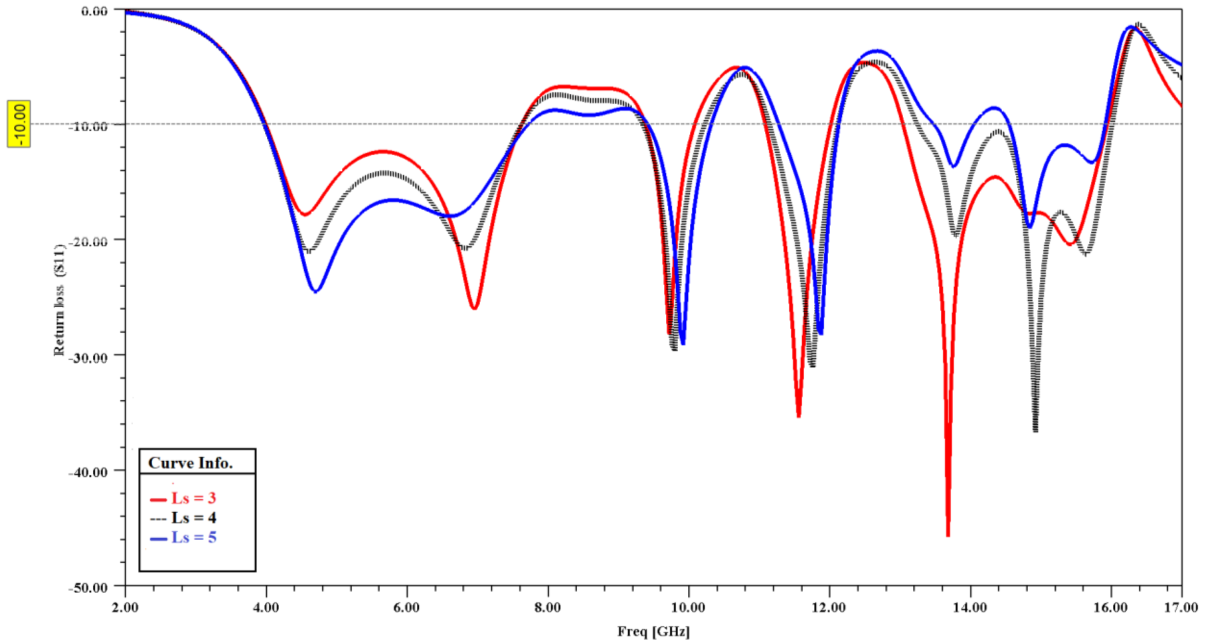

Fig.7 Simulated return loss S_{11} for the P-DRA with different values of the DGS length Ls.

5. References

1. **S. Peddakrishna., T. Khan., and A. De. (2017).** “Electromagnetic band-gap structured printed antennas: A feature-oriented survey,” International Journal of RF and Microwave Computer-Aided Engineering, vol. **27**, no. **7**, doi: 10.1002/mmce.21110.
2. **S. T. Low., & Z. Wu. (2007).** Microstrip-coupled rectangular dielectric resonator antennas on different substrates.
3. **B. Mukherjee., P. Patel., and J. Mukherjee. (2020).** “A review of the recent advances in dielectric resonator antennas,” Journal of Electromagnetic Waves and Applications, vol. **34**, no. **9**, pp. 1095–1158, doi: 10.1080/09205071.2020.1744484.
4. **D. Soren., R. Ghatak., R. K. Mishra., and D. R. Poddar. (2014).** “Dielectric resonator antennas: Designs and advances,” Progress In Electromagnetics Research B, vol. **60**, no. **1**, pp. **195–213**, doi: 10.2528/PIERB14031306.
5. **A. Gupta,. & R. K. Gangwar. (2020).** “Hybrid Rectangular Dielectric Resonator Antenna for Multiband Applications,” IETE Technical Review (Institution of Electronics and Telecommunication Engineers, India), vol. **37**, no. **1**, pp. **83–90**, doi: 10.1080/02564602.2019.1565961.
6. **S. Khan., H. Ali., R. Khan., S. N. K. Marwat., H. Ramenah., and C. Tanougast. (2019).** “Multi band Frequency Reconfigurable Dielectric Resonator Antenna for multiple wireless application,” 2019 2nd International Conference on Communication, Computing and Digital Systems, C-CODE 2019, pp. **73–76**, , doi: 10.1109/C-CODE.2019.8681011.
7. **N. K. Darimireddy., C. Wang Park., R. R. Reddy., and B. R. S. Reddy. (2019).** “Multi-band rectangular hybrid antennas loaded with inter-digital structure slot,” 2019 IEEE Indian Conference on Antennas and Propagation, InCAP 2019, pp. **1–4**, , doi: 10.1109/InCAP47789.2019.9134493.

8. **A. Sharma., & R. K. Gangwar. (2016).** "Compact triband cylindrical dielectric resonator antenna with circular slots for wireless application," Journal of Electromagnetic Waves and Applications, vol. **30**, no. **3**, pp. **331–340**, doi: 10.1080/09205071.2015.1114430.
9. **H. Elftouh., N. T. Amar., A. McHbal., A. Zakriti., and M. Elbakkali. (2019).** "Suppression of Harmonic of Microstrip Patch Antenna Using Defected Ground and Defected Microstrip Structure," Procedia Manufacturing, vol. **32**, pp. **653–660**, doi: 10.1016/j.promfg.2019.02.267.
10. **M. El-Sayed., A. Yossry., A. Yahia., M. El-Easser., and N. Gad. (2021).** "Printed monopole antenna design with parasitic element for multi-band applications," ICEEM 2021 - 2nd IEEE International Conference on Electronic Engineering, no. **July**, doi: 10.1109/ICEEM52022.2021.9480643.
11. **C. A. Balanis. (1997).** "Antenna Theory - Analysis And Design (Constantine A Balanis) (2Nd Ed).pdf."
12. **N. H. Gad., & M. Vidmar. (2018).** "Design of a Microstrip-Fed Printed-Slot Antenna Using Defected Ground Structures for Multiband Applications," vol. **33**, no. **8**, pp. **854–860**.
13. **R. K. Mongia., & P. Bhartia. (1994).** "Dielectric resonator antennas—a review and general design relations for resonant frequency and bandwidth," International Journal of Microwave and Millimeter-Wave Computer-Aided Engineering, vol. **4**, no. **3**, pp. **230–247**, doi: 10.1002/mmce.4570040304.
14. **N. Ioan., I. Andrei., T. Irina., R. Ionut., B. Gabriel., and N. Liviu. (2008).** High K dielectric resonator antenna, vol. **7**, no. **5**.